International Journal of Power Electronics and Drive System (IJPEDS)
Vol.3, No.4, December 2013, pp. 409 - 417
ISSN: 2088-8694

Performance of LED Employing Metal Oxide Mixed Thermal Interface Material by Structure Function Analysis

Subramani Shanmugan, Devarajan Mutharasu
Nano Optoelectronics Research Laboratory, School of Physics,
Universiti Sains Malaysia (USM), 11800, Minden, Pulau Pinang, Malaysia.

Article Info

Article history:

Received Aug 15, 2013
Revised Oct 16, 2013
Accepted Oct 28, 2013

Keyword:

EDAX analysis
Metal oxide
Thermal paste
Transient analysis

ABSTRACT

LED industries are currently focusing on the thermal management to reduce the junction temperature as well as the total thermal resistance for high power solid state lighting application. Metal powder or metal oxide filled thermal paste (TP) using as a thermal interface material is one kind of approach to solve the problem. In connection with that, milled TiO_2 and Cr_2O_3 powder were mixed in different ratio with commercial thermal paste. Cumulative structure function (CSF) analysis was used to characterize the metal oxide mixed thermal paste as thermal interface material (TIM) for 3W LED. TiO_2 mixed TIM showed good performance on reducing junction temperature (ΔT_J = 1.19 ºC) for driving current at 350 mA. Overall, TiO_2 mixed TP shows low value of board to heat sink thermal resistance ($R_{th\text{-}b\text{-}hs}$) compared to all other results. Energy Dispersive Spectrum (EDS) analysis results revealed the percentage of mixed powder as low when compared with mixed ratio. O_2 content in mixed paste showed immense effect on reducing total thermal resistance.

Corresponding Author:

Subramani Shanmugan
Nano Optoelectronics Research Laboratory, School of Physics,
Universiti Sains Malaysia (USM), 11800, Minden, Pulau Pinang, Malaysia.
Email: shagan77in@yahoo.co.in

1. INTRODUCTION

Standard machined surfaces are rough and wavy, leading to relatively few actual contact points between surfaces. The insulating air gaps created by multiple voids of “contacting” hard surfaces are simply too large a thermal barrier for even modest power applications. Yovanovich et al. [1] have calculated that simply replacing air with grease can reduce the thermal resistance by a factor of five or so (depending on the surfaces and contact pressure). Fillers must be introduced into the epoxy in order to provide good thermal transfer, because epoxies are insulators and very poor thermal conductors. The thermal conductivity of an epoxy will be determined by the choice of filler, the percentage of filler loading, and morphology of the filler particle; all of which play a critical role in the overall viscosity / rheology of the epoxy formulation. All modern TIMs are composites containing particulate fillers that push thermal conductivity up to the 7 W/m.K range. Inorganic particulate fillers include aluminum oxide, magnesium oxide, aluminum nitride, boron nitride, and diamond powder. Metal fillers, notably silver, are also used [2]. For this reason, thermally conductive epoxy adhesives have been formulated with very fine filler particles at moderate concentrations. Even further down the packaging hierarchy, epoxies have played a key role in board level assemblies; acting as encapsulates in advanced packaging techniques such as COB and TAB [3]; staking SMT components to PCB‟s [4];

No study has been reported so far related to the performance of other metal oxides as a filler material into TIM for LED packaging using structure function analysis using T3Ster equipment. This paper analyzes the performance of metal oxide powder on changing junction temperature (T_J) and total thermal resistance ($R_{th\text{-}tot}$) of 3W LED for various driving current. Cumulative structure function analysis has been used for this study.

2. EXPERIMENTAL METHOD

2.1 Preparation of metal oxide mixed Thermal paste

In this study, TiO_2 and Cr_2O_3 powders have been selected and well grinded using ball mill (Make: ROCKLABS Model: Bench Top Ring Mill) for about 1 hour and mixed with the alumina based commercial thermal paste (cooler master) as weight basis (approx.). The average particle size of powder was measured as 2.5 µm for TiO_2 and 2 µm for Cr_2O_3 using particle size analyzer. Alumina based TP was used as TIM. Mixing of powders with paste was done by manual mixing. Three different mixing ratios were used in this study as follows: 20 % : 80 %, 40 % : 60 % and 60 % : 40 %. In order to make 20 : 80 ratio, 1.6 g of TP was weighed (for 80 %) and mixed with 400 mg (for 20 %) of milled TiO_2 powder to make 2 g as total weight. For 40 : 60 ratio, 1.2 g of TP was weighed and mixed with 800 mg of milled TiO_2 powder. For 60 : 40 ratio, 800 mg of TP was weighed and mixed with 1.2 g of milled TiO_2 powder. The same methodology was followed to prepare for Cr_2O_3 mixed TP in this study. The sample name in the consecutive sections is denoted as follows: 20% TiO_2 mixed TP – 20TiO; 40% TiO_2 mixed TP – 40TiO; 60% TiO_2 mixed TP – 60TiO; 20% Cr_2O_3 mixed TP – 20CrO; 40% Cr_2O_3 mixed TP – 40CrO; and 60% Cr_2O_3 mixed TP – 60CrO. In this study, 3W green LED package attached with Metal Core Printed Circuit Board was used for all measurements and placed over the heat sink. The thermal transient curve of the LED is captured based on the electrical test method JEDEC JESD-51. The metal oxide mixed TIM is sandwiched between the 3W green LED and the commercial heat sink as show in Figure 1. The thermal behavior of the LED for metal oxide mixed TP is captured by the Thermal Transient Tester (T3Ster) in still air box.

The transient cooling curve was recorded for various driving current between 100 and 700 mA. EDAX analysis was also performed using HITACHI S-3400 model to study the elemental composition of the mixed TP. To measure the exact amount of elemental percentage, EDS measurement was done at more than 7 points for thoroughly mixed TP.

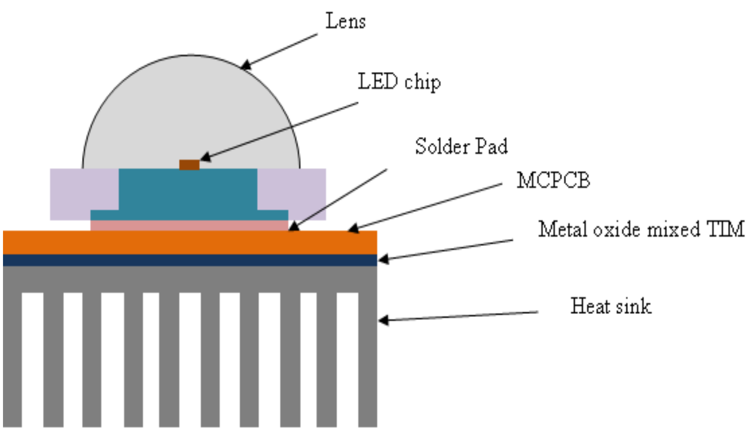

Figure 1. Schematic diagram of device under test showing metal oxide filled TIM sandwiched between LED package and heat sink

2.2 Structure Function Analysis

Structure functions are defined as a graphical representation of the RC-model of thermal systems. It was previously known as Protonotarios–Wing function [5]. Structure functions are generated using one main heat flow path which can be considered as a direct model of thermal system. The cumulative structure functions are generated from the Cauer-network equivalent RC model. It is a function of thermal capacitance versus thermal resistance. Cumulative structure function gives information on the volume of the material inside a package in which the heat spreads. Meanwhile, the derivative of cumulative structure function forms a function which is proportional to the area of the heat spreading cone. This derivative function is called differential structure function. Both cumulative and differential structure functions enable one to determine the partial thermal resistance of the heat flow path and the die attach failures inside a package [6].

2.3 K factor calibration

Before the real measurement, the LED was thermally calibrated using dry thermostat and T3Ster as the power supply. The product of K and the difference in temperature-sensing voltage (referred to as *ΔVF*) produces the device junction temperature rise:

$$\Delta T_J = \Delta V_F \, K \tag{1}$$

During the calibration process, the LED was driven with lower operating current at 1mA to prevent self heating effect at the junction. The ambient temperature of the LED was fixed to 25˚C and the voltage drop across the junction was recorded once the LED reaches thermal equilibrium with the temperature of the thermostat. Later, the ambient temperature of the LED was varied from 35˚C, 45˚C, 55˚C, 65ºC, 75˚C and 85˚C and the voltage drop across the junction was noted at each ambient temperature. From the calibration process, the K-factor of the LED was determined from the graph of junction voltage (voltage drop) against ambient temperature as shown in Figure 2.

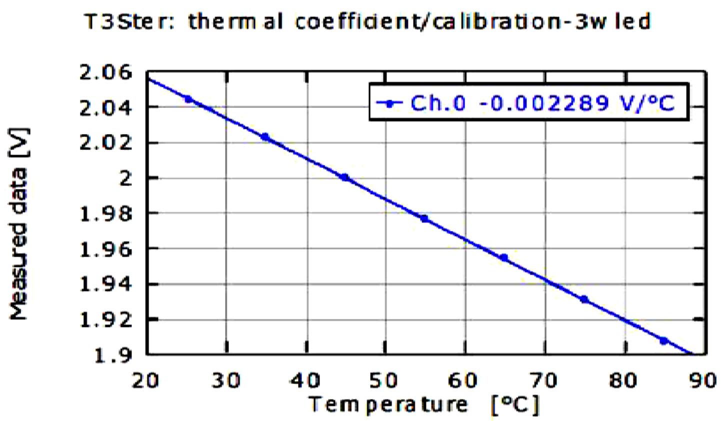

Figure 2. K factor calibration curve.

3. RESULTS AND DISCUSSION

3.1 Transient Curve Analysis

Cumulative structure function (CSF) is recorded for 3W green LED using metal oxide powder mixed thermal paste as TIM. We have recorded the cumulative structure function for various current ranges from 100 to 700 mA. We have selected only 3 current ranges for CSF analysis. Figure 3a shows that the CSF of 3W LED recorded at 100 mA driving current for different metal oxides mixed commercial TP as TIM. It clearly indicates that the TiO_2 mixed TP shows low $R_{th\text{-}tot}$ (Total thermal resistance) when compared to Cr_2O_3 mixed TP and unmixed TP. The circle in the Figure 3a shows some deviation on the curve and clearly depicts that it is due to the nature of powder used to mix with the TP. This deviation is may be due to the effect of thermal resistance of metal oxide mixed TP using as TIM. Figure 3a also clearly explains that the material content in mixed TP plays an important role on both reducing and increasing the $R_{th\text{-}tot}$ of the LED package. The CSF curve is also recorded for 350 mA and observed as given in Fig 3b. It depicts the influence of driving current on the $R_{th\text{-}tot}$ as decreasing with increasing current and also reveals that the 60TiO has low $R_{th\text{-}tot}$ than others. But we could not observe any deviation in the CSF curve as observed in 100 mA (Figure 3a). The difference in $R_{th\text{-}tot}$ observed as small for driving current 700 mA (Figure 3c) when compared to 100 and 350 mA. Transient cooling curve was used to measure the junction temperature of the 3W LED for various driving current. It is observed that the T_J value increases as the driving current increases for 3W LED using unmixed TP as TIM.

The Figure 4 shows the difference in Junction temperature rise (Δ T_J) from the results of unmixed TP with respect to driving current for various TiO_2 concentrations in TP. It reveals that the (- ve) negative sign seems to be the behavior of increase in T_J for driving current at and above 400 mA. It clearly indicates that the T_J reduces as driving current increases up to 350 mA. The figure 3 depicts that the change in T_J depends on not only the composition of TiO_2 powder and also the driving current.

As we know, the T_J increases as the current input to LED increases and reported in another work [7]. In our study, the powder mixed TP helps to reduce the T_J considerably for operating current less than 350 mA. 60TiO at 350 mA performed well in reducing T_J value by 1.19 ºC from unmixed TP and no considerable improvement in T_J reduction is observed for 40TiO for current up to 350 mA. Figure 4 also depicts that the T_J increases noticeably for driving current > 350 mA and especially for 40TiO mixed TP which shows immense effect on T_J reduction. The influence of Cr_2O_3 on changing the T_J is also discussed here and the observed values from CSF analysis are plotted against driving current as given in Figure 5. It shows the behavior as same as TiO_2 mixed TP and also shows that 20CrO and 40CrO show good performance on reducing the T_J for driving current up to 350 mA. But 60CrO powder mixed TP causes to increase the T_J substantially as the driving current increases from 400 to 700 mA when compared to other percentages. In addition to this, the change in thermal resistance (R_{th}) with respect to metal oxide concentration as well as the driving current are also studied and discussed here. The R_{th} values are derived from the CSF curves for all samples as given in Figure 6 (a-c) and Figure 7 (a-c).

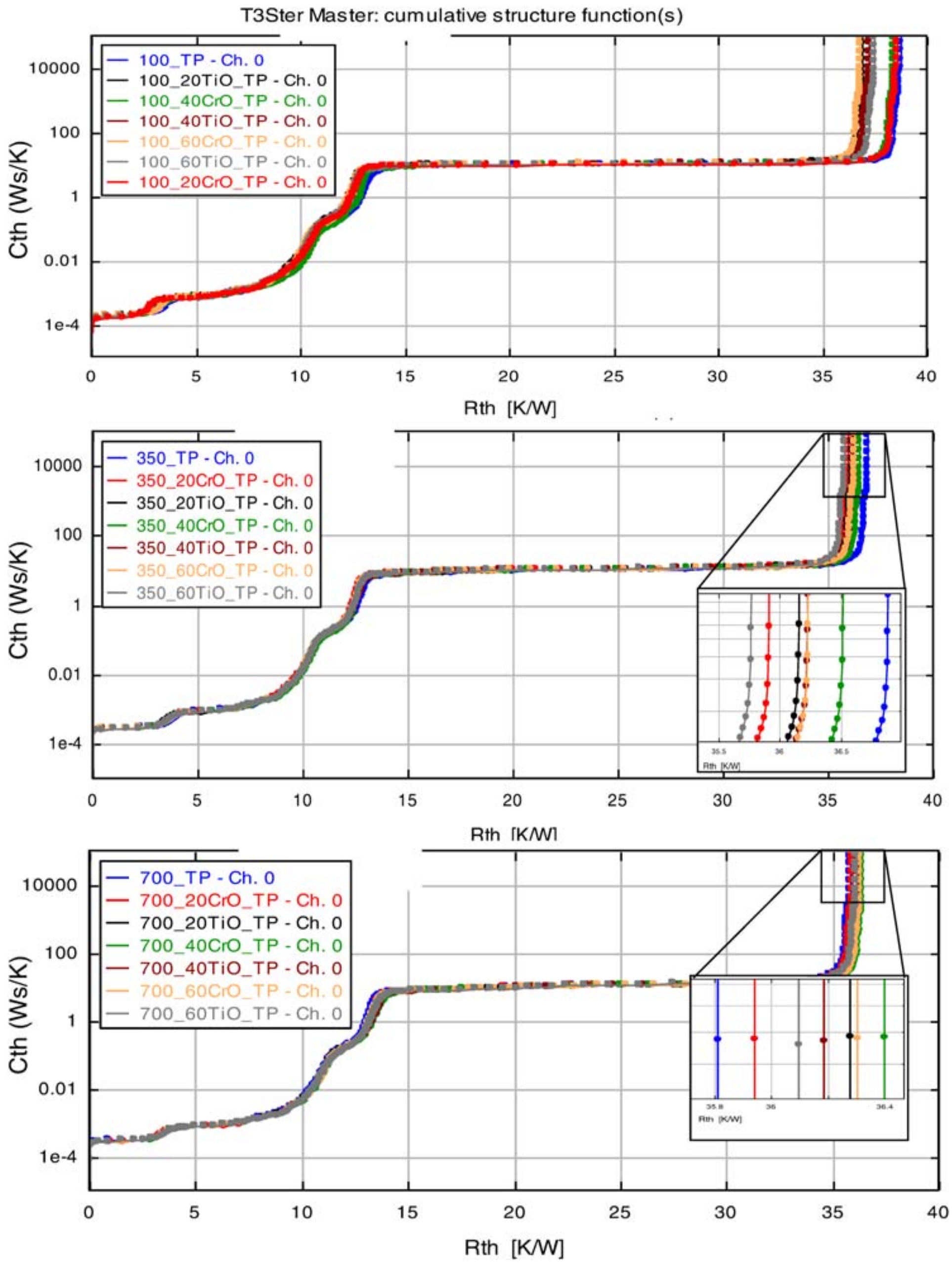

Figure 3 Cumulative Structure Function of 3W green LED for different metal oxide (TiO_2 and Cr_2O_3) mixed TIM measured at (a) 100 mA driving current, (b) 350 mA driving current and (c) 700 mA driving current

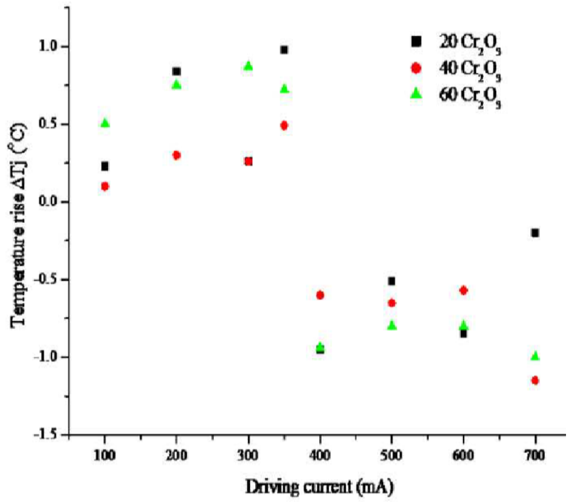

Figure 4. Variation in junction temperature rise for different TiO_2 concentration in TIM with respect to driving current

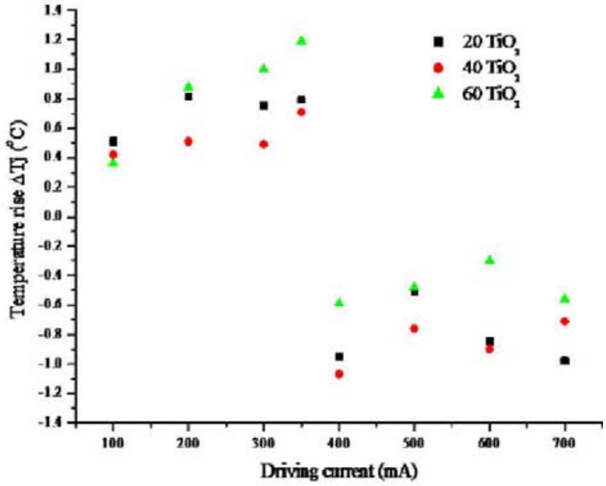

Figure 5. Variation in junction temperature rise for different in TIM with respect to driving current

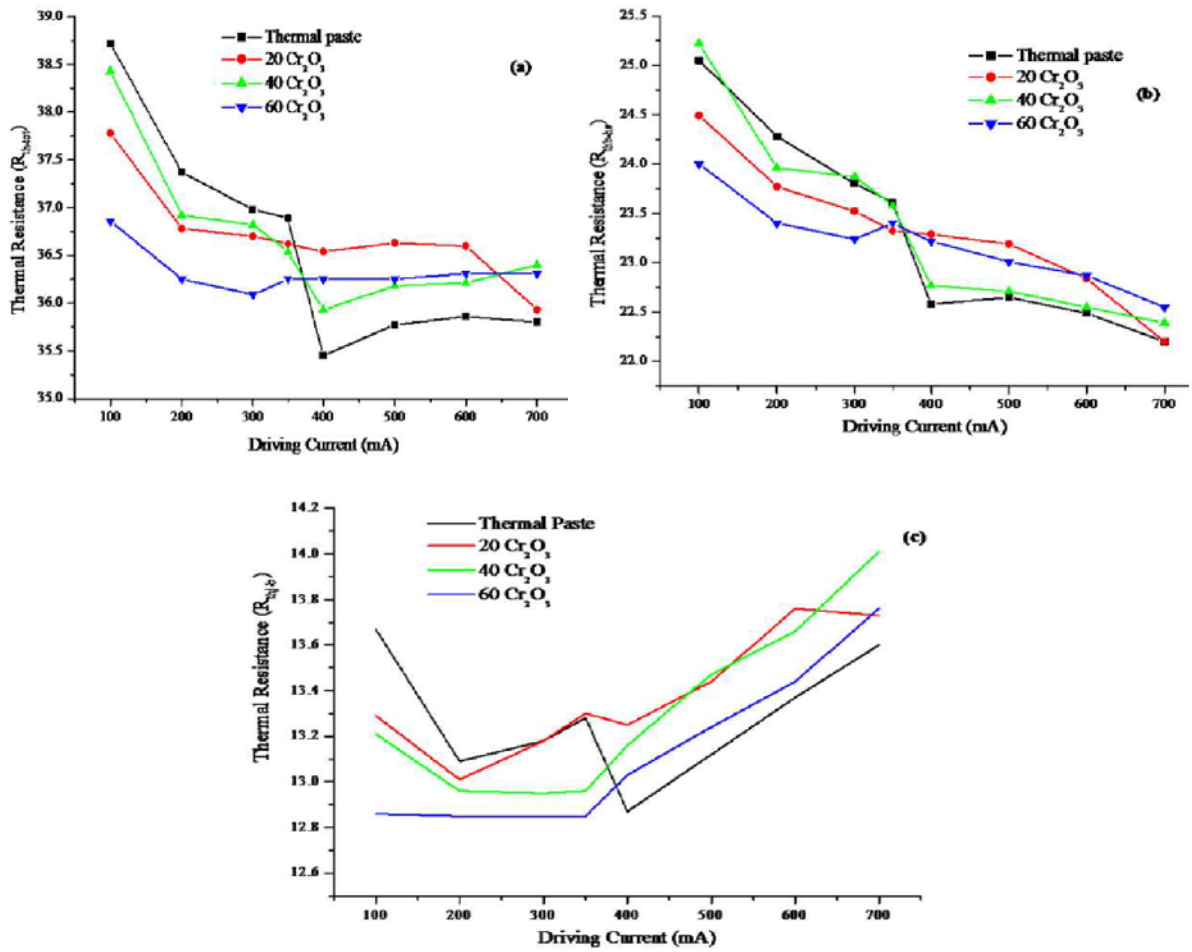

Figure 6. Change in (a) total thermal resistance ($R_{th\text{-}tot}$), (b) board to heat sink thermal resistance ($R_{th\text{-}b\text{-}hs}$) and (c) junction to board thermal resistance for various Cr_2O_3 concentrations at different driving current.

From the Fig.6 (a), $R_{th\text{-}tot}$ value considerably reduces for 60CrO up to 350 mA driving current especially for 100 mA (1.86 ºC/m.W) and there is no change could be observed even at higher driving current (form 400 to 700 mA). The Figure 6a clearly shows that the Cr_2O_3 mixed TP performs well for the driving current < 350 mA. In addition, the thermal resistance paths are similar for 40CrO when compared with unmixed TP and 20CrO are similar with 60CrO. Figure 6b shows the change in $R_{th\text{-}tot}$ as linear as the R_{th} reduces with driving current increases. From the Figure 6b, 40CrO has low R_{th} value than 20CrO and 60CrO for driving current at and above 400 mA. Fig.5c clearly explains the change in R_{th} from junction to board ($R_{th\text{-}j\text{-}b}$) for various Cr_2O_3 concentrations with respect to current. It shows that the $R_{th\text{-}j\text{-}b}$ is low when 60CrO used as Thermal Interface between heat sink and LED package. Since the rate of heat transfer changes with respect to composition of the material, the R_{th} value for junction to board also changes. Figure 6c clearly explains that 40CrO and 60 CrO as TIM reduces the $R_{th\text{-}j\text{-}b}$ considerably for driving current up to 350 mA. Moreover, the $R_{th\text{-}j\text{-}b}$ shows high value for Cr_2O_3 mixed TP than pure TP for driving current above 400 mA. It is attributed to the current crowding effect [8].

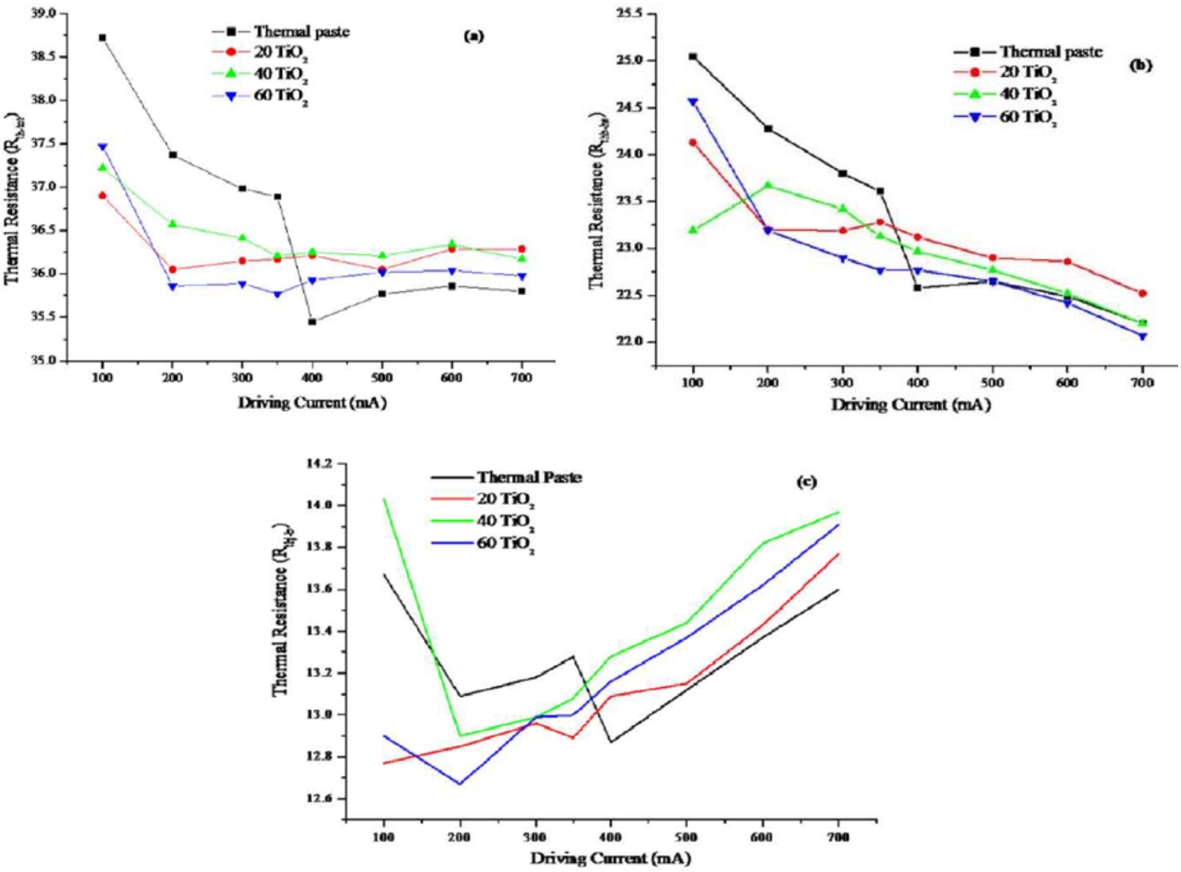

Figure 7. Change in (a) total thermal resistance ($R_{th\text{-}tot}$), (b) board to heat sink thermal resistance ($R_{th\text{-}b\text{-}hs}$) and (c) junction to board thermal resistance for various TiO_2 concentrations at different driving current

Figure 7a shows the change in $R_{th\text{-}tot}$ of 3W LED for various driving current where TiO_2 mixed TP used as TIM. TiO_2 mixed paste behaves same as observed for Cr_2O_3 but the values are different. As we observed for Cr_2O_3 mixed thermal paste, the $R_{th\text{-}tot}$ reduces as the driving current reduces up to 350 mA when compared to pure thermal paste. $R_{th\text{-}tot}$ value does not change for current from 200 mA to 700 mA. Especially, 60TiO performs well in reducing $R_{th\text{-}tot}$ for up to 350 mA driving current. In addition, 20TiO and 40TiO shows high value from 200 mA to 700 mA. Overall, TiO_2 mixed TP help to reduce the $R_{th\text{-}tot}$ of 3W LED for up to 350 mA. Figure 7b shows the R_{th} between board and heat sink. It clearly indicates that $R_{th\text{-}b\text{-}hs}$ obeys the same behavior of $R_{th\text{-}tot}$ and 60TiO shows immense effect on reducing the R_{th} between board and heat sink at and above 600 mA when compared to unmixed TP. Very low value in $R_{th\text{-}b\text{-}hs}$ (22.02 K/W) is observed with

60TiO when compared to Cr_2O_3 mixed TP. Overall, TiO_2 mixed TP shows low value of $R_{th\text{-}b\text{-}hs}$ compared to all other results observed in this study.

The measured junction to board thermal resistance ($R_{th\text{-}j\text{-}b}$) from cumulative structure function is given in Fig.7c. It shows that 20TiO shows linear behavior on $R_{th\text{-}j\text{-}b}$ for driving current from 100 mA to 700 mA. A drastic reduction from 14.3 K/W to 12.9 K/W could be observed for 40TiO when driving current increases from 100 mA to 200 mA. The Figure 7c also clearly indicates that an increase manner in $R_{th\text{-}j\text{-}b}$ is observed for 40TiO and 60TiO for driving current from 400 mA to 700 mA.

The increasing behavior of $R_{th\text{-}tot}$ for driving current above 500 mA for all results is mainly due to the current crowding phenomenon and hence the junction temperatures increases as with driving current increases. From the literatures, the current crowding takes place at high current densities in semiconductor devises [9, 10]. In other words, in the presence of a temperature gradient, energy is propagated through the lattice by these phonon waves [11]. If the atoms oscillated harmonically, the velocity of phonon waves would be the speed of sound in a crystal. However, anharmonicity is caused by higher order interactions among atoms, known as phonon scattering, which lead to a change in direction of the phonon wave [12]. It may be due to the presence of various metal atoms with different atomic sizes are present in the TP (O – 4.8 Å, Al – 11.8 Å, Zn – 14.2 Å, Ti – 17.6 Å, Cr – 16.6 Å). From the observed results, the inelastic scattering occurs and creates resistance to thermal transport and lowers the thermal conductivity.

This scattering can result from collisions of phonons with each other (Umklapp scattering) or defects in the crystal structure such as impurities (Zn and other atoms) and grain boundaries. Overall, an increase in thermal resistance for driving current at and above 400 mA could be observed for all metal oxide mixed TP as well as unmixed TP. It is attributed to the effect of Umklapp scattering, which is the dominant source of heat transfer resistance at ambient and higher temperatures [13]. The aim of the work was base on the increase of thermal conductivity by adding such metal oxides (Cr_2O_3 and TiO_2) into commercial alumina paste. The observed $R_{th\text{-}tot}$ of Cr_2O_3 (Fig.4a) and TiO_2 (Fig.5a) mixed TP was high at high operating current. Based on the results reported by Williams et. al., [14], a heavy atom in a light matrix scatters less effectively than a light atom in a heavy matrix. The atomic mass of Cr (52 atomic mass unit (amu)) and Ti (47.9 amu) is higher than Al (27 amu) and so the point defect relaxation times were different for Cr_2O_3 and TiO_2 mixed TP when compared with unmixed TP and hence the resistance varies for powder mixed TP. The observed results from CSF curve for $R_{th\text{-}b\text{-}hs}$ are indirectly representing the thermal conductivity behavior of the TIM material. The thermal conductivity of Al_2O_3, Cr_2O_3 and TiO_2 varies from 25.10 to 12.55, 9.99 to 32.94 and 6.69 W/m.K at 100 ºC respectively [15]. From our studies, the $R_{th\text{-}b\text{-}hs}$ were different with respect to the ratio of Cr_2O_3 and TiO_2 mixed into TP. The $R_{th\text{-}b\text{-}hs}$ for TiO_2 mixed TP increases for 20TiO and decreases as the concentration increases. In addition, the decreasing behavior of $R_{th\text{-}b\text{-}hs}$ with driving current increases shows contradict for the results observed as current crowding in GaN for high driving current [10]. The $R_{th\text{-}b\text{-}hs}$ for Cr_2O_3 mixed TP shows random changing with respect to driving current and Cr_2O_3 ratio. But the results of Cr_2O_3 are similar as observed from TiO_2 as $R_{th\text{-}b\text{-}hs}$ value decreases as the driving current increases with irrespective to the mixed ratio. These results show that the T_J helps to increase the conductivity of TiO_2 mixed TP as well as the Cr_2O_3 mixed TP by increasing the temperature of the mixture during measurement.

3.2 EDAX Analysis

The elemental composition of metal oxide mixed TP was also studied and plotted as given in Figure 8(a&b). The Figure 8 does not show the expected percentage of elements based on the mixed quantity. The exact reason for this difference could not be identified. Figure 8a shows the variation of elemental composition in TiO_2 mixed TP. It shows that Zn is detected as impure in the TP which may comes from unmixed TP as impure. It is evidently proved by observing Zn concentration in Cr_2O_3 mixed TP also. The decreasing behavior for Zn and Al may be due to the addition of metals such as Ti in TiO_2 mixed TP and Cr in Cr_2O_3 mixed TP. But it is observed that the oxygen concentration increases as the metal oxide powder mixed to TP. The increased oxygen content may be as a result of oxygen atom from TiO_2 and Cr_2O_3. Figure 8(a) shows that the Ti concentration increases as weight of TiO_2 powder mixed in TP increases. The increase in Ti in TP helps to reduce the T_J (ΔT_J – 1.19 ºC) for driving current 350 mA. But it is not supported to decrease the T_J as well for higher driving current. It also noticed that the T_J and $R_{th\text{-}tot}$ as well as the $R_{th\text{-}b\text{-}hs}$ values are low even Ti is observed as low when compared to Cr content in TP (Figure 8b). Moreover, at lower concentration of Ti (20TiO), the Zn concentration is high compared to all other elements in mixed TP. The results are almost same for Cr_2O_3 mixed TP as observed high Zn content. From Figure 8b, the oxygen content of the TP is also played an important role on reducing T_J as well as $R_{th\text{-}tot}$ when Cr_2O_3 mixed with TP. It shows that TiO_2 mixed TP shows good effect on reducing T_J as well as $R_{th\text{-}tot}$ even the O_2 content is high when compared to Cr_2O_3 mixed TP. In addition to that, the Cr content in the TP is high when compared to Ti content in TP though it is mixed with same weight basis.

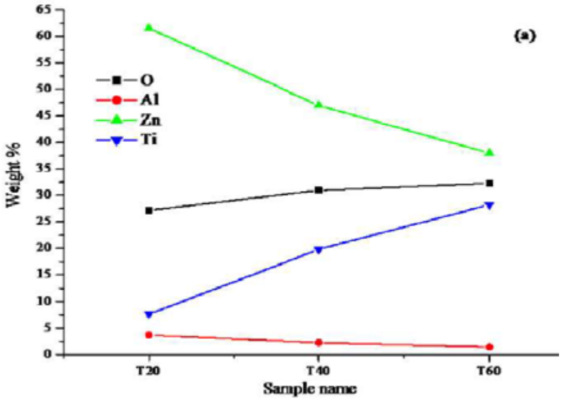

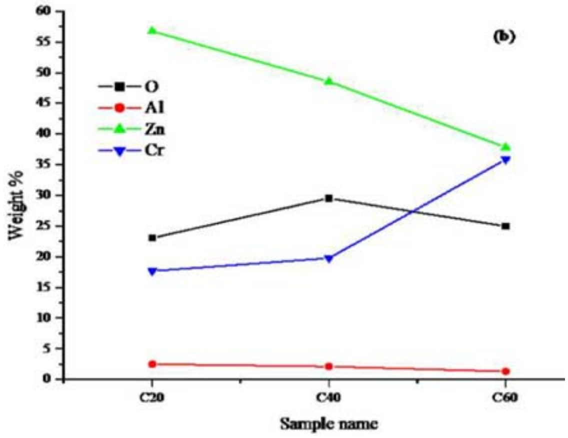

Figure 8. Elemental weight percentage available in (a) TiO_2 mixed TIM for different TiO_2 mixed ratio and (b) Cr_2O_3 mixed TIM for different TiO_2 mixed ratio.

4. CONCLUSION

Metal oxide powder mixed thermal paste was used as a TIM for high power LED and the thermal behavior was tested using CSF for different driving current. The total thermal resistance was varied with respect to Ti and Cr content as well as O_2 content in the thermal paste. TiO_2 mixed thermal paste performed well in reducing T_J for driving current up to 350 mA. TiO_2 mixed thermal paste showed good influence on reducing $R_{th\text{-}tot}$, $R_{th\text{-}b\text{-}hs}$ and also T_J for various Ti content with respect to current. Metal oxide power mixed TIM not influenced much on thermal behavior of 3W LED for driving current > 400 mA. The impurity in TIM also played an important role in changing the thermal resistance of the whole LED package. Cr_2O_3 powder did not support to enhance the TIM performance as compared to TiO_2 powder.

REFERENCES

[1] M.M.Yovanovich, J.R.Culham, and P.Teertstra, “Calculating Interface Resistance,” *Electro. Cooling,* vol. 3, pp. 24-29, May 1997
[2] http://www.electronics-cooling.com/2003/11/thermal-interface-materials/, Accessed on 15.2.2013
[3] J.Boutillier, R.Roche, “Chip Protection on Tape Automated Bonding,” *Proc. of SEMICON East*, Boston, MA, 1982
[4] F.W. Kulesza, R.H.Estes, “Conductive epoxy solves surface mount problems,” *Electronic Products*, March 1984
[5] E.N. Protonotarios, O.Wing, "Theory of Nonuniform RC Lines, Part II: Analytic Properties in the Time Domain,” *Proc. of IEEE Transactions on Circuit Theory*, vol. 14, pp. 13-20, March 1967.
[6] M.Rencz, A.Poppe, E.Kollar, S.Ress, V.Székely, “Increasing the accuracy of structure function based thermal material parameter measurements,” *Proc. of IEEE Trans. Compon. Packag. Technol.,* vol. 28, pp. 51-57, March 2005.
[7] P. Anithambigai, K. Dinash, D. Mutharasu, S. Shanmugan, C. K. Lim, “Thermal analysis of power LED employing dual interface method and water flow as a cooling system,” Thermochimica Acta, vol. 523, pp. 237-244, August 2011.
[8] A.J. Fischer, A.A. Allerman, M.H. Crawford, K.H.A. Bogart, S.R. Lee, R.J. Kaplar, W.W. Chow, S.R. Kurtz, K.W. Fullmer, and J.J. Figiel, “Room-temperature direct current operation of 290 nm light-emitting diodes with milliwatt power levels,” *Appl. Phys. Lett.* vol. 84, pp. 3394-3396, April 2004.
[9] M. Shatalov, A. Chitnis, P. Yadav, Md. F. Hasan, J. Khan, V. Adivarahan, H. P. Maruska, W. H. Sun, and M. Asif Khan, “Thermal analysis of flip-chip packaged 280 nm nitride-based deep ultraviolet light-emitting diodes,” *Appl. Phys. Lett.* Vol. 86, 201109, May 2005.
[10] G.H.B. Thompson, Physics of Semiconductor Laser Devices, John Wiley and Sons, 1980, pp.307-308.
[11] C.-L. Tien, A. Majumdar, F.M. Gerner, eds. Micro scale Energy Transport, Taylor & Francis, Washington D.C. 1998.
[12] C.-L. Tien, ed. Annual Review of Heat Transfer, Begell House, Inc: New York, 1996.
[13] M. P. Beck, Thermal conductivity of metal oxide nanofluids, Ph.D., Thesis, Georgia Institute of Technology, 14 -15, December 2008
[14] R. K. Williams, R. S. Graves, M. A. Janney, T. N. Tiegs, and D. W. Yarbrough, “The effects of Cr_2O_3 and Fe_2O_3 additions on the thermal conductivity of Al_2O_3,” *J. Appl. Phys.* Vol. 61, pp. 4894-4901, January 1987.
[15] J. F. Shackelford, W. Alexander, CRC Materials Science and Engineering Handbook, Ed. James F. Shackelford and W. Alexander, Boca Raton: CRC Press LLC, p. 283-284. 2001.